


Identification of the retrotalar pulley of the Flexor Hallucis Longus tendon

Chris Tzioupis¹  Anthony Oliveto,² Silke Grabherr,³ Jacques Vallotton¹ and Beat M. Riederer²

¹Medicol, Centre Orthopédique, Lausanne, Switzerland

²Plate-forme de Morphologie, Université de Lausanne, Lausanne, Switzerland

³Centre Universitaire Romand de Médecine Légale, Lausanne, Switzerland

Abstract

Functional Hallux Limitus is the expression of the gliding restraint of the Flexor Hallucis Longus (Fhl) tendon, resulting in several painful syndromes. This impingement is located along the tract of the Fhl tendon at the level of its retrotalar tunnel sealed posteriorly by a fibrous pulley. This pulley, although poorly anatomically characterized, has been arthroscopically proven that its presence or resection plays a pivotal clinical role in the biomechanics of the lower leg, being the main restraint to the physiological movement of the Fhl tendon. The aim of our study was to identify and characterize this anatomical structure. Eleven cadaveric lower legs were initially assessed by computer tomography (CT) imaging, subsequently plastinated, dissected and histologically evaluated by use of Mayer's and Hematoxylin stain. We have shown that the retrotalar pulley of the Fhl shares the same histological characteristics with the retinaculum of the long fibularis muscle and the retinaculum of flexor digitorum muscle, thus it constitutes a different entity than the adjacent formations.

Key words: CT; Fhl retinaculum; Flexor Hallucis Longus; Functional Hallux Limitus; histology; retrotalar pulley.

Introduction

Until now, the Flexor Hallucis Longus (Fhl) has been mostly described and referred to as a substitute muscle that plays a role in various augmentation surgical procedures (Ahmad et al. 2016). Its true functional morphology especially in its distal part is not thoroughly depicted even in anatomy books (Hicks, 1954; Frick, 1990; Rosse, 1997).

Furthermore, the variations of osseous anatomical relations, especially at the level of the rear foot, further complicate the efforts for its adequate and sufficient functional description (Tzioupis, 2013, 2014; Vallotton, 2014). The lack of its adequate anatomical description and relations has underscored its importance in the global kinetic chain of the lower extremity (Dananberg, 2000).

With the advents of rear foot arthroscopy (de Leeuw et al. 2009; Beals et al. 2010; Scheibling et al. 2017), we were able to better investigate the trajectory of the Fhl at a deeper level, as well as to explore the posterior subtalar joint in relation to the Fhl anatomy. The real-time acquisition of dynamic arthroscopic images allowed us to further understand the causes of various pathologies stemming

from the rear foot. It has been shown that these pathologies are biomechanically directly linked to the sagittal plane blockade caused by the Fhl tendon and its gliding restraint (Dananberg, 1986, 1988).

The existing literature highlighted the unfavorable results of conservative treatment regarding the pathologies linked to its restricted gliding (Bolgia & Boling, 2011). Thanks to our arthroscopic experience based on more than a thousand feet, we believe that the retrotalar tunnel is predominantly the anatomic area where the blockage of the normal tendon gliding occurs, and that one or more anatomical structures are involved in this process (Vallotton et al. 2010; Tzioupis, 2014).

Indeed, we were able to confirm the distinctive presence of a retinaculum-pulley-like formation posteriorly in the retrotalar tunnel bridging both posterior talar tubercles. This anatomical structure stabilized the tendon in the osseous gutter as digit pulleys in the hand (Vallotton et al. 2010). Its arthroscopic resection restored the normal Fhl glide, improved various biomechanical parameters of the forefoot, and has proven efficacious in the treatment of Fhl-related pathologies (Vallotton, 2014; Tzioupis, 2016).

To our knowledge, such a structure has never been adequately described in the anatomy books or has often been omitted. Our hypothesis was that there is a retrotalar pulley with distinctive anatomical characteristics other than those observed on the one existing beneath the sustentaculum tali. The aim of our study was to identify and describe this anatomical pulley formation in the retrotalar space.

Correspondence

Chris Tzioupis, Medicol, Centre Orthopédique, Av. Servan 4, CH-1006 Lausanne, Switzerland. E: ctzioupis@gmail.com

Accepted for publication 27 May 2019

Article published online 5 July 2019

Materials and methods

Anatomical specimens

The anatomical study was performed at the Platform of Morphology of the University of Lausanne, Switzerland. Eleven cadaveric lower leg specimens (five pairs and one single limb) and 11 cadaveric hand specimens were obtained by the local donation program numbered by pairs from 1 to 6 and subsequently examined. Each of the donors had given written consent prior to their demise. Our experiments were authorized by the ethical commission of the Canton Vaud, protocol 22/15 (*see Acknowledgements).

As described previously (Spinosa et al. 2009), in order to assure their preservation, corpses were perfused through the femoral artery with a mixture of 0.9 L of formaldehyde (38%), 0.5 L of phenol (85%), 1.0 L of glycerol (85%), 4.0 L of ethanol and 10.6 L of water. The bodies were stored at 8 °C until dissection. Eleven feet including ankle joints as well as 11 hands were preserved and used for imaging studies, dissection and histological analysis of retinacula. Characteristics of retrotalar groove and distance between posterior tubercles of talar bones were measured on the collection of female ($n = 11$) and male ($n = 17$) talar bones, at disposition at the Platform of Morphology of the University of Lausanne (Fig. 1a,b).

Computer tomography (CT) scan

Initially, the specimens were transferred to the University Centre of Legal Medicine (CURML) in order to perform an imaging assessment with a 64-multidetector CT scan Lightspeed Ultra VCT (eight rows; GE Medical Systems Milwaukee, WI, USA). Cadaver feet were positioned and scanned (Fig. 1c). Thereby, in order to allow standard radiological lecture of the obtained images, the feet were put in an anatomical position, allowing a scan from their distal to their proximal part. To maintain the feet in their position, Styrofoam blocks, normally used to maintain the patient's head, were used. The feet were fixed in this position by using fixation straps of the CT-table. For the scanning process, the following parameters were used: 120 kV; 200 mAs; field view interval, 0.7 mm, the thickness of section,

1.25 mm; and interval of reconstruction, 0.7 mm. The images acquired were then subjected to 3D reconstruction by using a commercial radiological lecture station (Advantage Windows, General Electrics), in order to adequately illustrate the trajectory of the various tendons and in particular those of the muscles of the Fhl and the Flexor Digitorum Longus. Anatomical areas of conflict or impingement were closely observed.

Plastination

Frontal sections through the foot were prepared for plastination, as described previously, and were used in preclinical teaching (Riederer, 2014).

Dissection

The Fhl was dissected from its proximal insertion on the fibula, to its insertion on the basis of the first phalanx of the hallux. Care was taken in order to protect the adjacent tissues, especially the pulleys of the tendons. The dissection was performed from the distal third of the gastrocnemius until the metatarsal heads, as well as the first phalanx of the hallux.

The standard surgical approach used during flexor tendon rupture repair was utilized for the dissection of A2 pulley of the middle finger of the cadaveric specimens (Samora & Klinefelter, 2016; Giesen et al. 2017).

Histology

The following tissue samples were harvested

Retrotalar pulley, retinaculum of the osteo-fibrous calcaneal tunnel of the Fhl beneath the sustentaculum tali, retinaculum of long fibularis muscle, retinaculum of the digit A2. The preparation of the samples was photographed and the tissue samples were tagged with a suture at their proximal ends for better orientation for histological preparation, and then placed in a solution of 50% ethanol.

The solution used consisted of the following agents

Chemicals: Ethanol puriss. p.a. 99.8%; Xylol; oil of cedar wood (VWR Chemicals, Dietikon, Switzerland); Paraffin

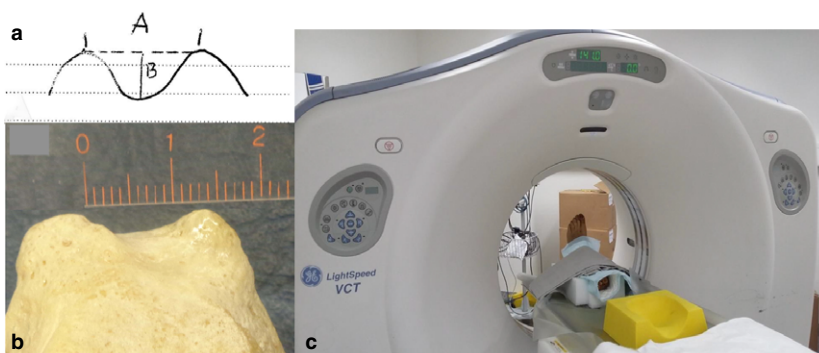


Fig. 1 (a,b) Characteristics of retrotalar groove and distance between posterior tubercles of talar bones. (c) Cadaver feet specimens were fixed with straps and a Styrofoam block in an anatomical position on a sliding table and scanned with a computer tomography (CT) Light Speed Ultra VCT (eight rows).

pastilles (Catalogue nr 107164, 56-58, Merck, Schaffhausen, Switzerland); Rotary Microtome HistoCore Biocut 2035 (Leica, Biosystems AG, Muttenz, Switzerland); Superfrost Plus Microscope slides (Thermo Fisher Scientific, Waltham MA, USA); Hematoxylin solution: Hematoxylin cryst 1% (Cl 75290, Merck Dietikon, Switzerland); Potassium alum 5% (Haenseler Swiss Pharma, Herisau, Switzerland); sodium iodate 0.2% (Merck, Dietikon, Switzerland); Citric acid anhydrous 1% (Fluka, Honeywell Research Chemicals, Reinach, Switzerland); Chloral hydrate 5% (Merck, Dietikon, Switzerland) in distilled water; Eosine-Y ready to use in 50% ethanol [Eosin Y (yellowish), BAKER ANALYZED®, J.T. Baker®]; Eukitt® Quick-hardening mounting medium (Fluka, Honeywell Research Chemicals, Reinach, Switzerland).

Samples were stained using Mayer's routine Hematoxylin and Eosin stain

[*Manual of Histologic Staining Methods* (ed. Luna Lee G). NY: McGraw Hill, 1960]. Briefly: on the first day, tissue was incubated in water (with several changes). On the second day, tissue was dehydrated with increasing ethanol concentrations in steps of 1–2 h incubations in 70% → 100%. Samples were kept for 24 h in cedar wood oil. On day 3, samples were incubated in liquid paraffin at 61 °C. On day 5, tissue was cut and oriented for longitudinal and cross-sectioning on wooden blocks. Seven-micrometer sections were mounted on Superfrost microscope slides and dried for 24 h.

Rehydration and Hematoxylin and Eosin staining (*see Acknowledgements): Slides were placed for 10 min in Xylol, 5 min each in decreasing concentrations of ethanol 100% → 95% → 70% → 40%, followed by 5 min in running tap water, staining for 10 min in Hematoxylin, then dehydrated by 5 min each in increasing steps of ethanol 40% → 70% → 95%. Slides were placed for 2 min in Eosin, 30 s in ethanol 95%, 1 min in ethanol 100%, and 10 min in Xylol. Slides were mounted with Eukitt and covered with a coverslip.

Brightfield images were acquired on an inverted microscope (Leica DMI8, Mannheim, Germany) equipped with a color digital CCD camera (DFC7000T, Leica). Objectives with 10× (HC PL Fluotar 10×/0.32) and 20× (HC PL FL L 20×/0.40) magnification were used.

Hematoxylin is a basic colorant that gives a blue to deep blue color, staining cytoplasm (ribosomes and nuclei, DNA/RNA) and basophilic components.

Eosin is an acidic colorant and stains basic proteins in a red to pink color, such as collagen fibers of connective tissue, ligaments, retinacula and tendons.

Results

CT scan

Eleven cadaveric legs underwent a CT scan in the CURML to further appreciate all the relevant adjacent structures

(osseous, tendinous or tissular). All scanned feet were reconstructed to demonstrate the passage of the tendon of the FHL. Two feet are represented in Fig. 2. As illustrated, several points of the FHL trajectory merit further attention: its retrotalar position, the passage under the sustentaculum tali, the crossing of the FHL and flexor digitorum longus at the level of the notch of Henry, and the trajectory of the FHL tendon between the two sesamoid bones. It is worth noting that in case of a developing Hallux Valgus deformity, the lateral sesamoid might be pushed laterally right into the metatarsal space.

Plastinated slices through the subtalar joint demonstrate the distinct passage of the tendon of the tibial posterior muscle, the flexor digitorum longus and the FHL underneath the sustentaculum tali (Fig. 3a,b). At higher magnification, the calcaneal osteo-fibrous trajectory of the FHL tendon beneath the sustentaculum tali can be depicted. Next to the tunnel, the neurovascular bundle passes in the calcaneus canal, covered by the abductor of the hallux.

Posterior tubercles of the talar bones showed considerable variability, with a mean distance between the two tubercles of 10.25 mm (8.5–12.5 mm) and retrotalar groove of 2.85 mm (1.5–4 mm) for both sexes (female $n = 11$, males $n = 17$).

Dissection

The dissecting technique was similar for all the specimens. The trajectory of the FHL muscle was followed from 30 cm above the calcaneal tuberosity until its distal insertion. The

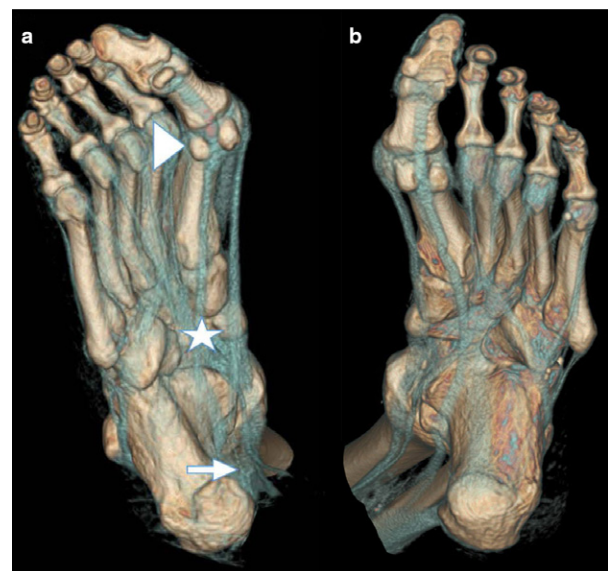


Fig. 2 3D-VR (volume rendering) reconstruction showing bony and tendinous structures of the scanned feet. Note the retrotalar trajectory of the Functional Hallux Limitus (FHL) tendon. (a) Right foot: note the formation of an additional sesamoid bone at the insertion point. Triangle: sesamoids; Star: notch of Henry; Arrow: retrotalar tunnel.

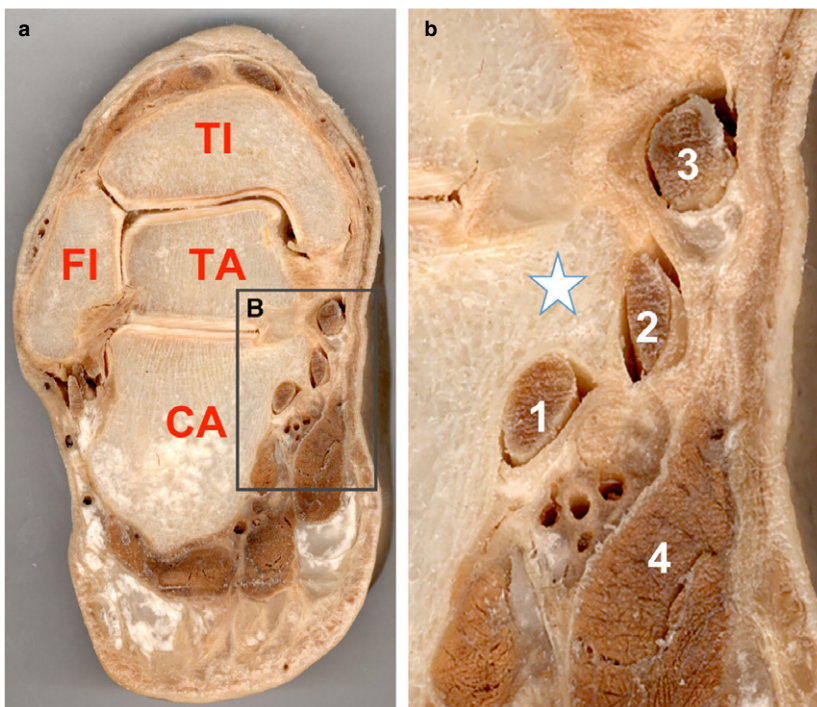


Fig. 3 (a,b) Plastinated frontal sections across the tibiotalar joint illustrate the passage of the Flexor Hallucis Longus (Fhl) underneath the sustentaculum tali. Note the conjunctive structure surrounding the osteo-fibrous canal and the proximity of the Fhl to the neurovascular bundle. (a) TI, tibia; FI, fibula; TA, talus; CA, calcaneus. (b) 1: Flexor Hallucis Longus; 2: Flexor Digitorum Longus; 3: Tibialis Posterior; 4: Abductor Hallucis; Star: Sustentaculum Tali.

bipennate texture of its fibers was macroscopically confirmed. Its tendon occupied nearly the whole length of the posterior surface of the muscle.

The trophicity of the muscle belly and the level of the musculo-tendinous junction, which was located above the retrotalar pulley, varied among the different specimens.

The Fhl tendon, below the lower end of the tibia, was guided in the retrotalar space passing in an osseous groove between the medial and lateral tubercles covered posteriorly in all specimens by a firm retinaculum: the retrotalar pulley. The depth of the tunnel varied among the specimens.

This pulley extended until the subtalar joint but not beneath it. At the calcaneal level beneath the sustentaculum tali, the retinaculum was totally different macroscopically, much thinner than the retrotalar pulley. Residing within the subtalar joint, a synovial meniscoid-like formation was observed and constitutes an additional reliable landmark between the talar and the calcaneal retinacula (Fig. 4).

We have macroscopically observed a major difference in the structure density of the retrotalar pulley compared with the looser conjunctive tissue colonized with blood vessels and the surrounding calcaneal osteo-fibrous tunnel under the sustentaculum tali. This was confirmed by histological observations.

Histology

Histological sections of the retrotalar pulley (Fig. 5) clearly show the presence of a dense, regular connective tissue (cut in cross- and longitudinal sections to demonstrate the thickness (cross-section 1–1.5 mm and 14–15 mm in length) of

the pulley, typically found in retinacula as well as in tendons. The transition from a dense to a looser arrangement towards the retinaculum of the osteo-fibrous tunnel beneath the sustentaculum tali was observed in dissections (Fig. 4), as well as in histological sections (Fig. 5a–c), with the presence of looser connective tissue, blood vessels and less dense collagen fibers.

In order to compare and investigate the presence of potential similarities in fiber composition and structure, the retinaculum of the fibularis longus muscle (Fig. 6) and the retinaculum of the flexor digitorum (A2; Fig. 7) were cut in cross- and longitudinal sections and analyzed for their histological composition. Both retinacula showed dense and regular fibrous tissue, with tightly packed, unidirectional and parallel arrangements of collagen fibers (Semisch et al. 2016). In addition, the retinacula were surrounded by loose conjunctive tissue and blood vessels. Histological arrangement of the pulley and retinacula was similar in all retinacula. Network density varied and was similar between the retrotalar pulley and A2 digit pulley.

Discussion

The aim of our study was to identify and characterize, by use of imaging and histology, the retrotalar retinaculum of the Fhl tendon at the level of the retrotalar tunnel. Our results confirmed our previous clinical and arthroscopic observations regarding the existence of a distinctive retrotalar Fhl pulley, with an identical structural organization as the A2 digit pulley.

Based on our histological results we have shown that the retrotalar pulley is different from the adjacent similar

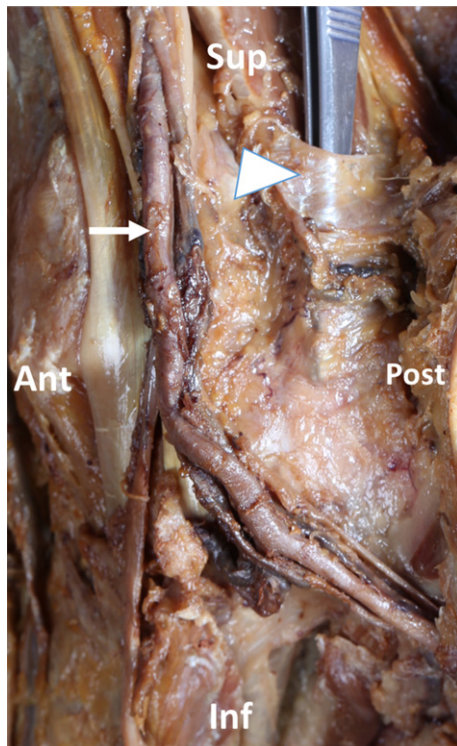


Fig. 4 Left medial view: dissection of retrotalar pulley and osteo-fibrous tunnel. The forceps replace the Flexor Hallucis Longus (Fhl) tendon. Note the trajectory of tendons and the saphena magnus vein. Sup, superior; Inf, inferior; Ant, anterior; Post, posterior; Triangle: retrotalar pulley; Arrow: tibialis posterior artery.

formations (i.e. the retinaculum of the fibro-osseous calcaneal tunnel beneath the sustentaculum tali), and bears similar histological characteristics to other retinacula.

Macroscopically, we showed that the retrotalar pulley extended until the subtalar joint but not beneath it. At the calcaneal level, the exposed retinaculum was totally different, that is much thinner than the retrotalar pulley. A transition zone was identified between the two formations, further confirming the differences in their consistency as well as in their function.

The retrotalar tubercles and the groove in between were defined by the variable eminence of tubercles. We have shown that the retrotalar pulley circumvents the tendon of the Fhl. It is identified as a 15-mm large band of 1.5 mm thickness of dense and regular connective tissue that restrains the entrance of tendon and muscle mass. The histology of this pulley corresponds to the composition of retinacula or tendons. At the transition from retrotalar to the sustentaculum tali canal, the content of surrounding tissue changes, and is more composed by finer and irregular collagen fibers, blood vessels and adipose tissue.

The following points could be perceived as limitations of our study.

Although the presence of the Fhl pulley was found in all 11 cadaveric specimens, this cadaveric population does not

allow for a statistical investigation regarding its incidence. However, this was not the aim of our study as this issue has been the purpose of several ongoing clinical trials that have been instigated by us.

The anatomical and radiological images were selected in a posteromedial plan in order to adequately reveal the relevant structures. The advantage of this orientation was the visualization of the Fhl and its tendon. However, the acquisition of the images and their reconstructions in a firm predefined position was impossible with the dissected feet because of the immobility of the cadaveric samples. Indeed, in the absence of rigidity, a predefined ankle position (for example 90°) would have facilitated the comparison between the specimens. Furthermore, the length of the Fhl tendon from its musculotendinous junction to the joint level could have been measured, as well as the ratio between this value and the tendon length from the ankle to its distal insertion on the phalanx of the hallux.

Given the paucity of the literature on the Fhl and its adjacent structures, it is essential to realize the importance of the retrotalar pulley (Hicks, 1953; Durrant & Chockalingam, 2009; Zammit et al. 2009; Vega et al. 2017).

The bipennate texture of the Fhl fibers was macroscopically confirmed during our study. The specific fiber texture underscores the pivotal role of this muscle in the conservation of the lower limb biomechanics, by exerting concentric and especially eccentric actions in specific gait cycle time-stamps. Therefore, the disturbance of its normal function results in a significant alteration in foot kinetics, which is followed by anatomically remote site complications (Hicks, 1956; McPoil & Knecht, 1985).

We have also observed that the trophicity of the belly muscle and the level of the musculotendinous junction, located above the retrotalar pulley, varied among the different specimens. Indeed, we were able to verify this finding by the dynamic images acquired during our arthroscopic treatment of Functional Hallux Limitus. A hypertrophic belly muscle as well as a lower musculotendinous junction, alone or in combination, were consistently associated with an Fhl blockage at the level of the retrotalar pulley.

Based on our ongoing clinical research, we have shown elsewhere the importance of the pulley as a contributing factor and biomechanical modifier in various lower leg pathologies (Vallotton, 2012; Tzioupis, 2013).

According to our experience based on our arthroscopic findings, the Fhl gliding restraint can be attributed to a disproportionate size between its tendon and the surrounding pulley (Tzioupis, 2014).

Additionally, we have highlighted a significant change in the distribution of plantar pressures before and after endoscopic tenolysis of the pulley of the Fhl tendon. After the intervention, a restoration of the applied load of the first metatarsal head at the end of the stance phase has been clearly observed on foot scan platforms (Tzioupis, 2016).

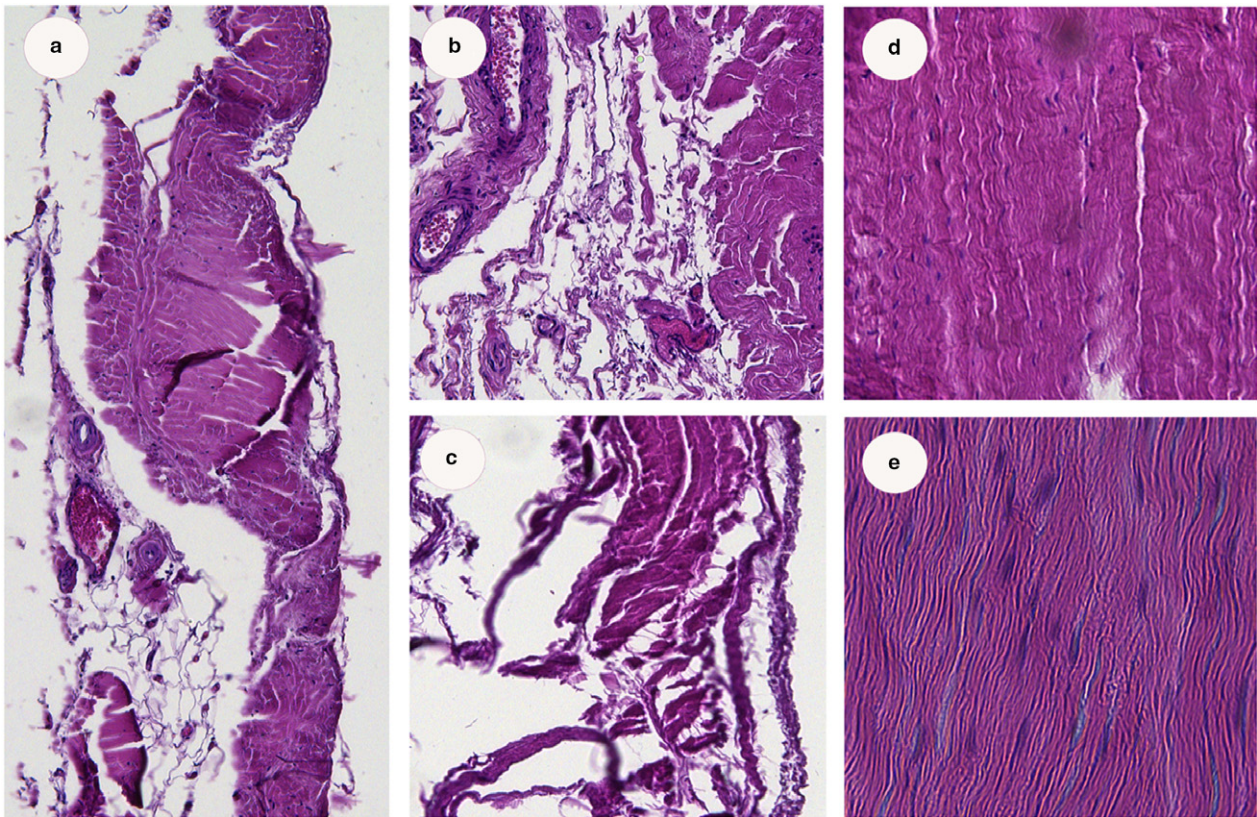


Fig. 5 (a–e) Histology of retrotalar pulley in cross- (a–c) (magnification 10×) and longitudinal sections (d,e) (magnification 20×). At the retrotalar region, fibers are more dense, while near the osteo-fibrous calcaneal tunnel more blood vessels are found and collagen fibers are less dense (confirmed by surgical observations).

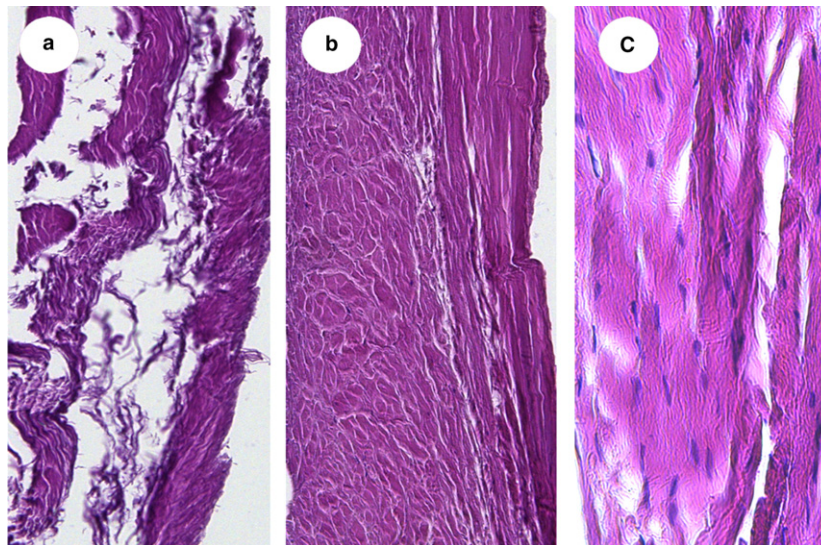


Fig. 6 (a–c) Cross- (a,b) and longitudinal sections (c). (magnification 10×: a,b; 20×: c). Histology of the inferior retinaculum of the long fibularis muscle. Note that the fibrous fibers have different trajectories.

Facing the talocalcaneal joint line, we have also identified the existence of a synovial ‘meniscoid’ structure on the medial side of the joint. This synovial structure protrudes outside of the joint by exerting traction in the

axis of the leg and by swaying the calcaneus. This manoeuvre increases the retrotalar space and restores the passage of the FHL tendon through its pulley (Vallotton et al. 2010).

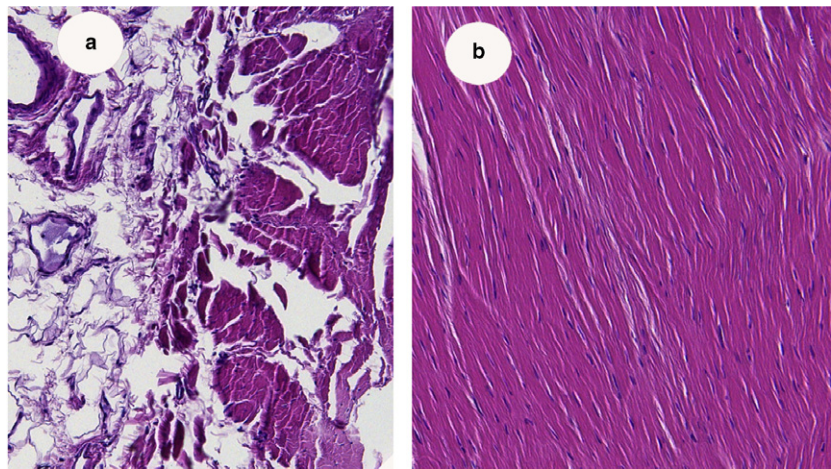


Fig. 7 (a,b) Histology of the pulley of the A2 (magnification 10 \times). Note that connective tissue is closely linked with ligaments to assure vascularization of retinaculi.

Furthermore, we revealed the histological similarities between the Fhl pulley and the A2 digit pulley with regard to their functional involvement.

The digital flexor sheath is a complex structure through which the flexor tendons of the fingers run. The sheath is essential for the normal function of the flexor tendons, it holds the flexor tendons close to the bone allowing them to effectively 'turn a corner' and transfer the force developed in the muscle-tendon unit into a movement of the phalanges (Lui et al. 2010).

The retinacular portion of the sheath consists of fibrous tissue condensations that wrap around the flexor tendons. These condensations are the flexor tendon pulleys. The A2 and A4 pulleys are true osteo-fibrous pulleys (they insert into bone), and are the strongest pulleys withstanding the greatest forces during pinch and grasp (Giesen et al. 2017).

In conclusion, the Fhl retrotalar pulley shares the same histological characteristics as the A2 pulley surrounding the digits, thus constituting a totally different anatomical entity as compared with similar adjacent structures. The clinical importance of this pulley is evident. Its texture, localization and relation to adjacent structures, along which it constitutes a functional unity, has to be clearly identified because of Fhl's biomechanical functional implications. Further clinical studies are warranted in order to further delineate the remaining questions pertaining to the anatomically functional importance of the Fhl pulley.

Acknowledgements

The authors thank the staff of CURML for scanning the anatomical specimens (Prof. Alexander Dominguez). *Parts of this study were the thesis work of Anthony Oliveto 'Etude anatomique du carrefour postérieur formé par le tendon du muscle long fléchisseur de l'hallux et la poulie rétro-talienne', at the faculty of Biology and Medicine, University of Lausanne. The authors would like to thank Mrs Irène Riederer and Ms Amandine Rindlisbacher for their excellent technical work in the preparation and staining of histological sections, The Cellular Imaging Facility (CIF) and Dr Jean-Yves Chatton

and Dr Jannick Kremp for their help in histological image acquisition. The authors would also like to thank Dr Pierrick Dijoux and Dr Cédric Charpilloz for their help during the dissection of the cadavers.

References

- Ahmad J, Jones K, Raikin SM (2016) Treatment of chronic achilles tendon ruptures with large defects. *Foot Ankle Spec* **9**, 400–408.
- Beals TC, Junko JT, Amendola A, et al. (2010) Minimally invasive distraction technique for prone posterior ankle and subtalar arthroscopy. *Foot Ankle Int* **31**, 316–319.
- Bolgia LA, Boling MC (2011) An update for the conservative management of patellofemoral pain syndrome: a systematic review of the literature from 2000 to 2010. *Int J Sports Phys Ther* **6**, 112–125.
- Dananberg HJ (1986) Functional hallux limitus and its relationship to gait efficiency. *J Am Podiatr Med Assoc* **76**, 648–652.
- Dananberg HJ (1988) The kinetic wedge. *J Am Podiatr Med Assoc* **78**, 98–99.
- Dananberg HJ (2000) Sagittal plane biomechanics. American Diabetes Association. *J Am Podiatr Med Assoc* **90**, 47–50.
- Durrant B, Chockalingam N (2009) Functional hallux limitus: a review. *J Am Podiatr Med Assoc* **99**, 236–243.
- Giesen T, Calcagni M, Elliot D (2017) Primary flexor tendon repair with early active motion: experience in Europe. *Hand Clin* **33**, 465–472.
- Frick H (1990) *Wolf-Heidegger's Atlas of Human Anatomy*. Basel: S. Karger Publishers.
- Hicks JH (1953) The mechanics of the foot I. The joints. *J Anat* **87**, 345–357.
- Hicks JH (1954) The mechanics of the foot. II. The plantar aponeurosis and the arch. *J Anat* **88**, 25–30.
- Hicks JH (1956) The mechanics of the foot. IV. The action of muscles on the foot in standing. *Acta Anat (Basel)* **27**, 180–192.
- de Leeuw PA, van Sterkenburg MN, van Dijk CN (2009) Arthroscopy and endoscopy of the ankle and hindfoot. *Sports Med Arthrosc Rev* **17**, 175–184.
- Lui TH, Chan KB, Chan LK (2010) Cadaveric study of zone 2 flexor hallucis longus tendon sheath. *Arthroscopy* **26**, 808–812.

- McPoil TG, Knecht HG** (1985) Biomechanics of the foot in walking: a function approach. *J Orthop Sports Phys Ther* **7**, 69–72.
- Riederer BM** (2014) Plastination and its importance in teaching anatomy. Critical points for long-term preservation of human tissue. *J Anat* **224**, 309–315.
- Rosse C, Gaddum-Rosse P, Hollinshead WH** (1997) *Hollinshead's textbook of anatomy*. Philadelphia:Lippincott-Raven Publishers.
- Samora JB, Klinefelter RD** (2016) Flexor tendon reconstruction. *J Am Acad Orthop Surg* **24**, 28–36.
- Scheibling B, Koch G, Clavert P** (2017) Cadaver study of anatomic landmark identification for placing ankle arthroscopy portals. *Orthop Traumatol Surg Res* **103**, 387–391. Epub 2017 Mar 1.
- Semisch M, Hagert E, Garcia-Elias M, et al.** (2016) Histological assessment of the triangular fibrocartilage complex. *J Hand Surg Eur* **41**, 527–533.
- Spinosa JPBE, Laurençon J, Kuhn G, et al.** (2009) Differential staged reflexes allow a localization of pudendal neuralgia. *Pelvipereineology* **28**, 24–28.
- Tzioupis C** (2013) A Multi-Segment Model Study to Evaluate the Sagittal Plane Blockade in Patients with Functional Hallux Limitus (FHL): Results after Endoscopic Tenolysis of the Flexor Hallucis Longus at the Retrotallar Pulley. 14th Congress of the European Federation of National Associations of Orthopaedics and Traumatology (EFORT), Istanbul, Turkey, 5-8 June 2013, Poster Presentation.
- Tzioupis C, Diehl S, Vallotton J** (2014) Flexor Hallux Limitus (FHL) as a potential predisposing factor for Anterior Knee Pain Syndrome (AKPS). A Prospective Cohort Study. 15th Congress of the EFORT, London, UK, 4–6 July 2014. Oral presentation.
- Tzioupis C** (2016) Functional Hallux Limitus (FHL). Implications on Anterior Cruciate Ligament (ACL) Ruptures. A new therapeutic approach. Oral presentation, 17th Efort Congress, Geneva, Switzerland, 1–3 June 2016.
- Vallotton J** (2012) Sagittal plane blockade in patients with Functional Hallux Limitus (FHL); results after endoscopic tenolysis of the Flexor Hallucis Longus tendon by use of a multi-segment model. A prospective comparative study. *ESSKA Congress*, Geneva, 3–6 May 2012.
- Vallotton J** (2014) Functional hallux limitus (Fhl): a new explanation for overuse pathologies. *Rev Med Suisse* **10**, 2333–2337.
- Vallotton J, Echeverri S, Dobbelaere-Nicolas V** (2010) Functional hallux limitus or rigidus caused by a tenodesis effect at the retrotalar pulley: description of the functional stretch test and the simple hoover cord maneuver that releases this tenodesis. *J Am Podiatr Med Assoc* **100**, 220–229.
- Vega J, Redo D, Savin G, et al.** (2017) Anatomical variations of flexor hallucis longus tendon increase safety in hindfoot endoscopy. *Knee Surg Sports Traumatol Arthrosc* **25**, 1929–1935.
- Zammit GV, Menz HB, Munteanu SE** (2009) Structural factors associated with hallux limitus/rigidus: a systematic review of case control studies. *J Orthop Sports Phys Ther* **39**, 733–742.